DOI: 10.1002/chem.200700005

Luminescent Nanocrystals for Nonenzymatic Glucose Concentration Determination

Leyu Wang and Yadong Li*[a]

Abstract: By using a facile, wet-chemical approach, luminescent $LaF_3:Ce^{3+}/Tb^{3+}$ single-crystal nanoparticles were prepared from nitrate and sodium fluoride precursors in a mixture of ethanol and ethylene glycol. These nanoparticles were functionalized with glucose. A novel fluorescence resonance energy transfer method for nonenzymatic glucose determination has been developed by using these glucose-modified nanocrystals. Under the chosen conditions, concentrations of glucose between 0.5 and 25.0 mmol L^{-1} in aqueous solutions were successfully determined. Owing to their high luminescence and good dispersibility in water, these nanocrystals are also potential fluorescent biolabels for other biological and clinical applications, such as in fluorescence imaging and for immunoassays.

Keywords: FRET (fluorescence resonance energy transfer) · glucose · luminescence · nanostructures

Introduction

The detection of glucose is very important in several fields, such as in food analysis, bioreactor monitoring, and clinical diagnosis. Diabetes is a common chronic disease, whose clinical detection and therapy is one of the major health care problems affecting lots of people all over the world.[1] Some noninvasive technologies for glucose detection have been developed,[2,3] however, to date, owing to the high demand for reliability and sensitivity, clinical diabetes monitoring has been mainly based on blood glucose measurements.[4] Recently, numerous attempts have been made to develop new glucose determination methods,[5–10] such as those involving electrochemical[11,12] and fluorescent[13,14] technologies. Some of these methods involve using the enzyme glucose oxidase,[5,15] and show excellent sensitivity and high selectivity, however, they also suffer from low stability owing to the intrinsic nature of the enzyme. Other glucose determination methods are based on the novel electrical properties of gold nanoparticles,[16] which have been widely used in biotechnology.[17] Among these technologies, fluorescent methods have attracted much interest, nevertheless, most of these are mainly based on fluorescent dyes.[7,18] However, few reports of a nonenzymatic method to determine glucose concentration by using luminescent rare-earth fluoride nanocrystals have been described.

In recent years, rare-earth fluoride nanocrystals have attracted growing interest for use as luminescent biolabels owing to their novel luminescent properties, which include long lifetimes, high quantum yields, low photobleaching, and high chemical stability.[19–24] However, to the best of our knowledge, the use of water-soluble and highly luminescent LaF_3 nanocrystals for glucose determination has not yet been reported. In this work, we have successfully synthesized water-soluble $LaF_3:Ce^{3+}/Tb^{3+}$ nanocrystals that emit luminescence in the green region with good crystallinity and high luminescence by using a facile, wet-chemical approach without the addition of surfactants. A novel fluorescence resonance energy transfer (FRET) technology for glucose determination has been developed based on FRET from glucose-modified $LaF_3:Ce^{3+}/Tb^{3+}$ nanocrystals to rhodamine B isothiocyanate (RhBITC) that had been conjugated with 3-aminophenyl boronic acid (APBA) (Figure 1).

Results and Discussion

$LaF_3:Ce^{3+}/Tb^{3+}$ nanocrystals were prepared without any surfactants by using nitrate and sodium fluoride as precursors in a mixture of ethylene glycol and ethanol. Figure 2 shows low- and high-resolution transmission electron microscope (TEM, HRTEM) images of the nanocrystals. The

[a] L. Wang, Prof. Dr. Y. Li
Department of Chemistry
Tsinghua University
Beijing, 100084 (P.R. China)
Fax: (+86) 10-6278-8765
E-mail: ydli@tsinghua.edu.cn

Supporting information for this article is available on the WWW under http://www.chemeurj.org/ or from the author.

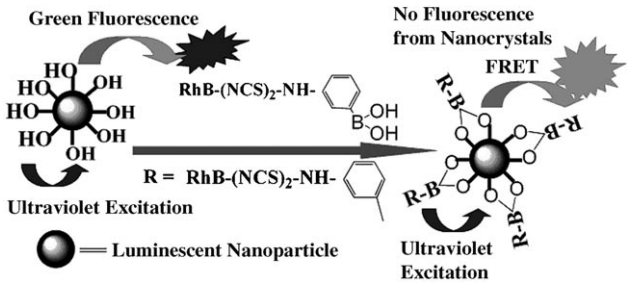

Figure 1. Schematic representation of the FRET system for glucose determination.

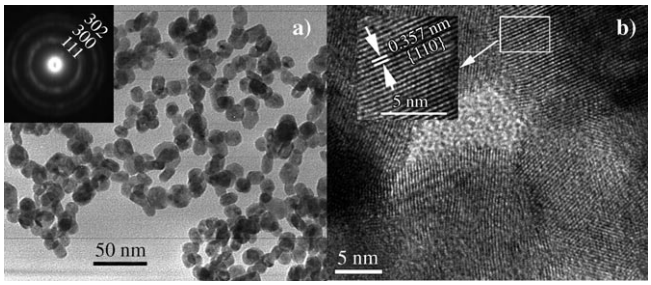

Figure 2. a) Low- and b) high-resolution TEM images of LaF_3:Ce(5%)/Tb(5%) nanoparticles. The inset of (a) shows the electron diffraction analysis.

TEM image shows that the nanoparticles possess good dispersibility and high crystallinity (inset of Figure 2a), with an average size of about 15–20 nm. The HRTEM image, which displays lattice fringes for the nanoparticles, indicates that the as-prepared nanoparticles are single crystals. Their good crystallinity, which is very beneficial to the high luminescence, was also identified by using X-ray diffraction (XRD) analyses. The XRD pattern of the as-prepared LaF_3:Ce^{3+} (5%)/Tb^{3+}(5%) nanocrystals is shown in Figure 3. All peak positions and relative intensities were in agreement with those of the hexagonal phase structure of the bulk LaF_3 crystal (JCPDS card no. 72-1435) with crystal cell parameters of $a=0.7163$ and $c=0.7329$ nm.

To the best of our knowledge, owing to low vibrational energies and the subsequent minimization of the quenching of the excited state of lanthanide ions, lanthanum fluoride is advantageous as a luminescent host material.[25,26] Furthermore, it is known that Ce^{3+} ions have a relatively broad absorption band from $\lambda=200$ to 300 nm with an allowed 4f–5d transition, and that they also undergo energy transfer to other rare-earth ions, in particular with Tb^{3+} ions for green emission.[25,27] Hence, in this work, we prepared LaF_3 nanocrystals co-doped with Ce^{3+}–Tb^{3+} ion pairs to obtain green luminescent biolabels. Moreover, the effects of the concentration of doped Ce^{3+} on the fluorescence intensity, centered at $\lambda=543$ nm, have also been demonstrated, and the results are given in Figure 4. The crystallinity and phase

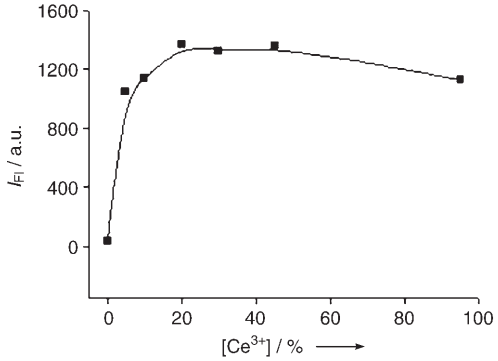

Figure 4. Effects of Ce^{3+} concentration on the fluorescence intensity of the nanoparticle powder (a.u.: arbitrary units).

purity of the as-prepared nanocrystals with different Ce^{3+} concentrations have been investigated by using XRD (see Figure S1 in the Supporting Information). Figure 4 shows that when the concentration of Ce^{3+} is zero then the as-prepared nanoparticles, that is, LaF_3:Tb^{3+}, emit very weak, green fluorescence. However, the as-prepared nanocrystals emit strong, green fluorescence when doped with 5% Ce^{3+}, whereas the fluorescence intensities fluctuate weakly when the concentration of Ce^{3+} increases from 5 to 95% (CeF_3/Tb^{3+}). Therefore, a concentration of 5% for the Ce^{3+} ions was adopted in this work.

Figure 5 shows the excitation and emission spectra of the LaF_3:Ce(5%)/Tb(5%) colloids dispersed in water. The col-

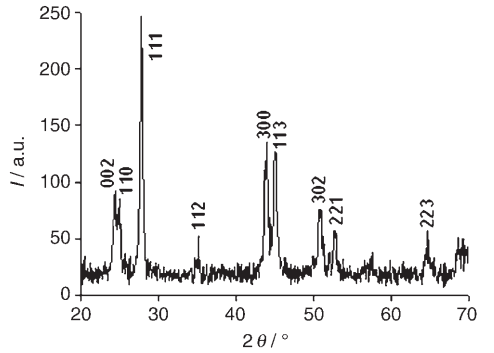

Figure 3. XRD pattern of the LaF_3:Ce(5%)/Tb(5%) nanoparticles.

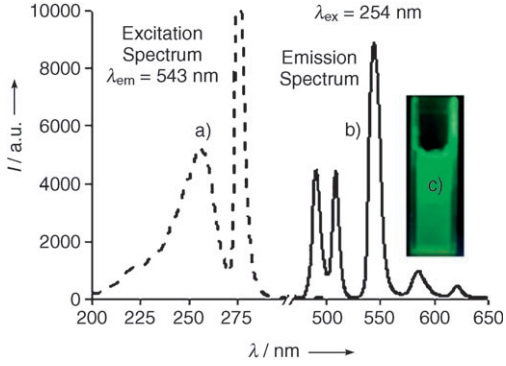

Figure 5. a) Excitation and b) emission spectra of LaF_3:Ce(5%)/Tb(5%) colloids. c) The luminescent photograph obtained under a UV lamp.

loidal solution possesses a broad excitation band from $\lambda =$ 200 to 300 nm, which is in good agreement with the absorption band of Ce^{3+} ions.[25] However, the main excitation is located at $\lambda = 254$ nm, whereas the strong peak at around $\lambda = 275$ nm in the excitation spectrum is a result of light scattering whose wavelength is about half that of the main emission at $\lambda = 543$ nm. Consequently, an excitation wavelength of $\lambda = 254$ nm was used throughout this work. Typical emissions for Tb^{3+} ions, which are clearly depicted in Figure 5b, can be attributed to the transitions for $^5D_4$–$^7F_6$ ($\lambda = 486$ nm), $^5D_4$–$^7F_5$ ($\lambda = 543$ nm), $^5D_4$–$^7F_4$ ($\lambda = 587$ nm), and $^5D_4$–$^7F_3$ ($\lambda =$ 619 nm), respectively.[22] The dominant green band emission is centered at $\lambda \approx 543$ nm. Additionally, it is worth noting that the peak at $\lambda \approx 511$ nm in the emission spectrum is a second light-scattering event instead of an emission peak, whose wavelength is double that of the excitation at $\lambda =$ 254 nm. The green emission of the colloids visible with the naked eye also is demonstrated in Figure 5c with the photograph obtained under irradiation from a UV lamp.

Although these highly luminescent LaF_3 nanocrystals can be easily dispersed in water or ethanol, they should be modified with appropriate organic compounds for specific binding to target molecules before they can be used for biological or chemical applications. It is known that boronic acid derivatives can be specifically bound to glucose through the interaction between the boronic acid group and *ortho*-dihydroxy groups,[8,28,29] as shown in Figure 1. Therefore, the luminescent nanocrystals were functionalized with glucose. The nanocrystals were alternately deposited with poly(allylamine hydrochloride) (PAH) and poly(sodium 4-styrenesulfonate) (PSS) by using a layer-by-layer strategy,[24] before the negatively charged nanoparticles (LaF_3/PAH/PSS) were modified with positively charged chitosan. Finally, the nanocrystals (LaF_3/PAH/PSS/chitosan) were modified with glucose through the Schiff base group (C=N) based on the interaction between the amine group on the nanoparticles and the aldehyde group on glucose. The functionalization of the LaF_3 nanocrystals (LaF_3–glucose) was characterized by means of FTIR spectroscopy (Figure 6). The spectrum was assigned as follows: The broad band at $\tilde{\nu} = 3439$ cm^{-1} is characteristic for the O–H stretching vibration, the peak at $\tilde{\nu} =$ 3034 cm^{-1} was attributed to the =C–H stretching vibration in the PSS benzene ring, and the transmission band at $\tilde{\nu} =$ 2924 cm^{-1} was assigned to the asymmetric stretching vibration of methylene ($-CH_2$). The weak bands at $\tilde{\nu} = 1601$, 1552, 1473, and 1414 cm^{-1} result from the C=C vibrations of the aromatic skeleton of PSS. The bands at $\tilde{\nu} = 1188$ and 1126 cm^{-1} were assigned as C–N stretching vibrations, whereas the bands at $\tilde{\nu} = 1034$ cm^{-1} were attributed to C–O stretching vibrations. The bands at around $\tilde{\nu} = 773$ and 673 cm^{-1} were attributed to C–H bending vibrations of the PSS benzene ring. Consequently, the FTIR results indicated that the surface modification of the nanocrystals was successful.

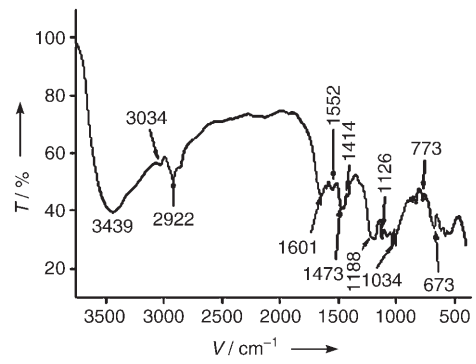

Figure 6. FTIR spectrum of the functionalized nanocrystals.

The unique spectroscopic properties of LaF_3 nanocrystals make them particularly suitable as FRET donors. It is well known that the FRET strategy[8,24,30–32] is very sensitive technology and is ideal for bioanalysis that is free from complicated separation steps, in which the fluorescence intensity is extremely sensitive to the separation distance between the donor and acceptor. Herein, the luminescent LaF_3 nanocrystals were used as the energy donor in the FRET system for glucose determination. A prerequisite of FRET is that the excitation band of the energy acceptor should have a large overlap with the emission band of the donor. Therefore, we chose RhBITC as the energy acceptor, which possesses good excitation ($\lambda \approx 558$ nm) at around the main emission of the LaF_3:Ce^{3+}/Tb^{3+} nanocrystals ($\lambda \approx 543$ nm). It should be noted that RhBITC should be conjugated with APBA to bind to glucose to form the boronic acid-functionalized energy acceptor (RhBITC–APBA). Figure 7 shows the excitation and emission spectra of RhBITC–APBA, along with the FRET results for LaF_3–glucose and RhBITC–APBA. Figure 7a shows the dominant excitation at $\lambda = 558$ nm, and also weak excitation bands between $\lambda = 220$ and 450 nm. It should be noted that the band at $\lambda = 292$ nm results from light scattering as opposed to being an excitation peak. Under excitation at $\lambda = 254$ nm, the LaF_3–glucose colloids display a strong, green emission at $\lambda = 543$ nm, whereas the spectrum for RhBITC–APBA is dominated by an emission at $\lambda = 584$ nm of moderate intensity. However, by mixing the LaF_3–glucose colloids with RhBITC–APBA, the green emission of the colloids at $\lambda = 543$ nm was sharply quenched by RhBITC–APBA through FRET. On the other hand, the yellowish-green fluorescence of RhBITC–APBA at $\lambda = 584$ nm was greatly enhanced, which strongly indicated that the FRET between LaF_3–glucose colloids and RhBITC–APBA was successful.

To test the nanocrystals, this FRET strategy was applied to the detection of glucose in an aqueous solution. Different volumes of glucose solution were introduced into a solution of LaF_3–glucose and RhBITC–APBA, and the solution was thoroughly mixed. About half an hour later, the fluorescence intensity of the emission band at $\lambda = 584$ nm was recorded. The amount of RhBITC–APBA bound to the surface of the LaF_3–glucose nanoparticles decreased in a stepwise manner as the amount of free glucose added to the system increased, as a result of the competitive binding between free and bound glucose on LaF_3 nanocrystals contain-

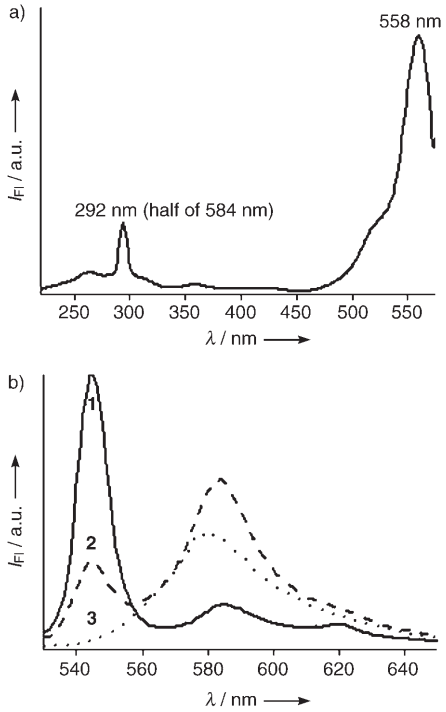

Figure 7. a) Excitation spectrum of RhBITC–APBA and b) emission spectra of colloids (LaF_3–glucose) (1), FRET system (LaF_3–glucose + RhITC–APBA) (2), and RhBITC–APBA (3). An excitation wavelength of $\lambda = 254$ nm was used for all detections. The excitation spectrum of RhBITC–APBA was obtained under an emission wavelength of $\lambda = 584$ nm.

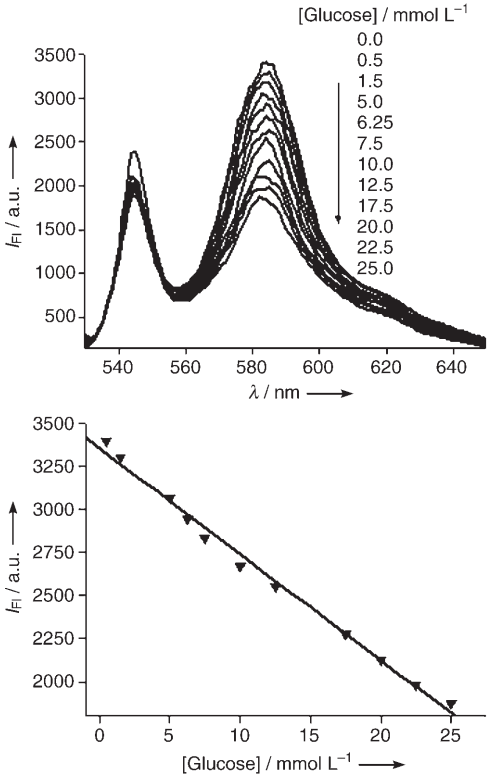

Figure 8. a) Fluorescence spectra of the detection system with different glucose concentrations and b) the linear relationship profile of fluorescence intensity versus glucose concentration.

ing boronic acid groups; this resulted in quenching of the fluorescence at $\lambda = 584$ nm. In other words, the addition of free glucose to the system widened the separation distance between the donor and acceptor, and led to a decrease of the FRET efficiency and subsequent fluorescence quenching. Consequently, the fluorescence response signal of the FRET system is an effective indicator of the glucose concentration. Figure 8 shows the detection results and the calibration graph (Figure 8b). As shown in Figure 8a, the intensity of the yellowish-green emission at $\lambda = 584$ nm gradually decreases with increasing glucose concentrations. The fluorescence intensity has a linear relationship to the glucose concentration over a glucose concentration of 0.5 to 25.0 mmol L^{-1}.

Conclusion

In summary, we prepared luminescent LaF_3:Ce^{3+}/Tb^{3+} single-crystal nanoparticles by using a facile, solvothermal strategy. Thereafter, these highly luminescent nanocrystals were functionalized with glucose for use as fluorescence labels for glucose determination. By using glucose-modified nanocrystals as the energy donor and APBA-modified RhBITC as the energy acceptor, a simple and sensitive nonenzymatic method for determining glucose concentration by using FRET technology has been successfully developed. The results described herein show a promising step towards rapid and sensitive detection of trace glucose in aqueous solutions. Furthermore, these luminescent nanocrystals are also potential fluorescent biolabels for use in other biological and clinical applications, such as in fluorescence imaging and for immunoassays.

Experimental Section

Chemicals and reagents: Analytical grade $La(NO_3)_3{\cdot}6H_2O$, $Ce(NO_3)_3{\cdot}6H_2O$, $Tb(NO_3)_3{\cdot}6H_2O$, NaF, ethylene glycol, ethanol, and glucose were obtained from Beijing Chemical Reagent. Deionized water was used throughout. Chitosan, RhBITC, and APBA were purchased from Sigma. PAH (Mw, 8000–11000) from Aldrich and PSS (Mw 13400) from Fluka were used as received. The chitosan solution (0.01 mg mL^{-1}) was obtained by means of dissolving chitosan (1.0 mg) and acetic acid anhydrate (1.5 mL) in deionized water and diluting the solution to 100 mL.

Synthesis of LaF_3 nanocrystals: LaF_3:Ce^{3+}/Tb^{3+} nanocrystals with an average diameter of 15–20 nm were synthesized by using facile, solvothermal technology. $La(NO_3)_3$ (1.8 mL, 0.5 mol L^{-1}), $Ce(NO_3)_3$ (100 μL, 0.5 mol L^{-1}), $Tb(NO_3)_3$ (100 μL, 0.5 mol L^{-1}), and sodium fluoride solution (3 mL, 1.0 mol L^{-1}) were added to a mixture of ethanol (20 mL) and ethylene glycol (10 mL), and the solution was thoroughly stirred. Subsequently, the milky colloidal solution was transferred to a 50 mL Teflon-lined autoclave and heated at 180 °C for 12 h. The system was then allowed to cool to room temperature. The final product was collected by means of centrifugation, washed once with ethanol and twice with deionized water to remove any possible remnants, and then dried at 60 °C for

8 h. Other nanoparticles with different dopant concentrations of Ce^{3+} were also prepared according to the same procedure.

Characterization: The phase purity and crystallinity of the samples were characterized by using a Bruker D8-advance X-ray powder diffractometer with $Cu_{K\alpha}$ radiation ($\lambda = 1.5418$ Å). The size and morphology of the as-prepared nanocrystals was observed at 100 kV by using a JEOL JEM-1200EX transmission electron microscope (TEM) and at 200 kV by using a JEOL JEM-2010F high-resolution transmission electron microscope (HRTEM). Luminescence spectra were recorded by using a Hitachi F-4500 fluorescence spectrophotometer with a xenon lamp source. FTIR spectra were recorded by using a Nicolet 560 spectrophotometer.

Modification of nanoparticles: LaF_3:Ce^{3+}/Tb^{3+} nanocrystals (0.1 g) were dispersed into deionized water (30 mL) by means of ultrasonication, then the colloids were fabricated with a polyelectrolyte to form the LaF_3/PAH/PSS core–shell structure according to our reported procedure.[23,24] Thereafter, LaF_3/PAH/PSS colloids were dispersed into water (40 mL) before chitosan solution (1.0 mL, 0.01 mg mL^{-1}) was added dropwise with vigorous stirring. The chitosan-coated nanocrystals were obtained by adding $NH_3 \cdot H_2O$ (150 μL, 28 %) to induce chitosan aggregation. The resulting powder was collected by means of centrifugation and washing with water. Nanoparticles functionalized with amine groups were further modified with glucose to obtain LaF_3–glucose nanocrystals. The chitosan-coated nanoparticles were dispersed into ethanol (40 mL) before glucose (150 mg) and triethylamine catalyst (150 μL) were added and the solution was stirred. Subsequently, the mixture was transferred into a 50 mL Teflon-lined autoclave and heated at 80 °C for 4 h. The LaF_3–glucose nanocrystals were purified by means of centrifugation, washing, and dispersion into deionized water by means of ultrasonication to form a colloidal solution. The final concentration of the colloids was fixed at 4 mg mL^{-1} prior to use.

Conjugation of rhodamine B isothiocyanate: To act as the energy acceptor, RhBITC should be conjugated to APBA to obtain a specific group, that is, a boronic acid group, for specific binding to *ortho*-dihydroxy groups on glucose. Typically, APBA (0.01 mmol) and RhBITC (0.01 mmol) were dissolved in ethanol (3 mL), and then diluted to 100 mL by adding deionized water and stirred for 72 h at room-temperature. The solution of APBA-functionalized RhBITC (RhBITC–APBA) was stored in the dark at 4 °C prior to use.

Determination of glucose: We used the functionalized nanoparticles to detect glucose with the change of the relative fluorescence intensity of the system. LaF_3–glucose colloids (150 μL, 4 mg mL^{-1}), RhBITC–APBA (100 μL, 0.1 mmol L^{-1}), and glucose solution (0.05 mol L^{-1}) were added to a 1.0 mL volumetric flask, diluted to 1.0 mL with phosphate buffer solution (25.0 mmol L^{-1}, pH 7.4), and then mixed thoroughly. After 30 min, the relative fluorescence intensity of the system was measured at $\lambda_{em} = 585$ nm ($\lambda_{ex} = 254$ nm).

Acknowledgements

This work was supported by the NSFC (90606006), the Foundation for the Author of National Excellent Doctoral Dissertation of China, and the State Key Project of Fundamental Research for Nanoscience and Nanotechnology (2006CBON0300).

[1] P. W. Barone, R. S. Parker, M. S. Strano, *Anal. Chem.* **2005**, *77*, 7556–7562.
[2] M. Paranjape, J. Garra, S. Brida, T. Schneider, R. White, J. Currie, *Sens. Actuators A* **2003**, *104*, 195–204.
[3] V. L. Alexeev, S. Das, D. N. Finegold, S. A. Asher, *Clin. Chem.* **2004**, *50*, 2353–2360.
[4] T. Koschinsky, L. Heinemann, *Diabetes/Metab. Res. Rev.* **2001**, *17*, 113–123.
[5] E. S. Forzani, H. Q. Zhang, L. A. Nagahara, I. Amlani, R. Tsui, N. J. Tao, *Nano Lett.* **2004**, *4*, 1785–1788.
[6] Y. H. Lin, F. Lu, Y. Tu, Z. F. Ren, *Nano Lett.* **2004**, *4*, 191–195.
[7] J. T. Suri, D. B. Cordes, F. E. Cappuccio, R. A. Wessling, B. Singaram, *Angew. Chem.* **2003**, *115*, 6037–6039; *Angew. Chem. Int. Ed.* **2003**, *42*, 5857–5859 .
[8] D. B. Cordes, S. Gamsey, B. Singaram, *Angew. Chem.* **2006**, *118*, 3913–3916; *Angew. Chem. Int. Ed.* **2006**, *45*, 3829–3832.
[9] M. Morikawa, N. Kimizuka, M. Yoshihara, T. Endo, *Chem. Eur. J.* **2002**, *8*, 5580–5584.
[10] S. Hrapovic, J. H. T. Luong, *Anal. Chem.* **2003**, *75*, 3308–3315.
[11] T. Chen, K. A. Friedman, I. Lei, A. Heller, *Anal. Chem.* **2000**, *72*, 3757–3763.
[12] T. J. Ohara, R. Rajagopalan, A. Heller, *Anal. Chem.* **1994**, *66*, 2451–2457.
[13] M. Wu, Z. H. Lin, M. Schaferling, A. Durkop, O. S. Wolfbeis, *Anal. Biochem.* **2005**, *340*, 66–73.
[14] M. Wu, Z. H. Lin, A. Durkop, O. S. Wolfbeis, *Anal. Bioanal. Chem.* **2004**, *380*, 619–626.
[15] X. D. Yan, X. H. K. Xu, H. F. Ji, *Anal. Chem.* **2005**, *77*, 6197–6204.
[16] B. K. Jena, C. R. Raj, *Chem. Eur. J.* **2006**, *12*, 2702–2708.
[17] S. J. Park, A. A. Lazarides, C. A. Mirkin, P. W. Brazis, C. R. Kannewurf, R. L. Letsinger, *Angew. Chem.* **2000**, *112*, 4003–4006; *Angew. Chem. Int. Ed.* **2000**, *39*, 3845–3848.
[18] D. B. Cordes, A. Miller, S. Gamsey, Z. Sharrett, P. Thoniyot, R. Wessling, B. Singaram, *Org. Biomol. Chem.* **2005**, *3*, 1708–1713.
[19] Y. W. Zhang, X. Sun, R. Si, L. P. You, C. H. Yan, *J. Am. Chem. Soc.* **2005**, *127*, 3260–3261.
[20] S. Sivakumar, P. R. Diamente, F. C. van Veggel, *Chem. Eur. J.* **2006**, *12*, 5878–5884.
[21] J. W. Stouwdam, F. van Veggel, *Nano Lett.* **2002**, *2*, 733–737.
[22] L. Y. Wang, Y. D. Li, *Nano Lett.* **2006**, *6*, 1645–1649.
[23] L. Y. Wang, Y. D. Li, *Chem. Commun.* **2006**, *16*, 2557–2559.
[24] L. Y. Wang, R. X. Yan, Z. Y. Huo, L. Wang, J. H. Zeng, J. Bao, X. Wang, Q. Peng, Y. D. Li, *Angew. Chem.* **2005**, *117*, 6208–6211; *Angew. Chem. Int. Ed.* **2005**, *44*, 6054–6057.
[25] P. R. Diamente, R. D. Burke, F. van Veggel, *Langmuir* **2006**, *22*, 1782–1788.
[26] Z. L. Wang, Z. W. Quan, P. Y. Jia, C. K. Lin, Y. Luo, Y. Chen, J. Fang, W. Zhou, C. J. O'Connor, J. Lin, *Chem. Mater.* **2006**, *18*, 2030–2037.
[27] K. Kompe, H. Borchert, J. Storz, A. Lobo, S. Adam, T. Moller, M. Haase, *Angew. Chem.* **2003**, *115*, 5672–5675; *Angew. Chem. Int. Ed.* **2003**, *42*, 5513–5516.
[28] W. Q. Yang, X. M. Gao, B. H. Wang, *Med. Res. Rev.* **2003**, *23*, 346–368.
[29] S. Gamsey, J. T. Suri, R. A. Wessling, B. Singaram, *Langmuir* **2006**, *22*, 9067–9074.
[30] A. R. Clapp, I. L. Medintz, J. M. Mauro, B. R. Fisher, M. G. Bawendi, H. Mattoussi, *J. Am. Chem. Soc.* **2004**, *126*, 301–310.
[31] I. L. Medintz, A. R. Clapp, H. Mattoussi, E. R. Goldman, B. Fisher, J. M. Mauro, *Nat. Mater.* **2003**, *2*, 630–638.
[32] X. D. Song, J. Nolan, B. I. Swanson, *J. Am. Chem. Soc.* **1998**, *120*, 11514–11515.

Received: January 3, 2007
Published online: February 26, 2007

